High-Pressure Adsorption Equilibria of Methane and Carbon Dioxide on Several Activated Carbons

Shuji Himeno,* Toshiya Komatsu, and Shoichi Fujita

Department of Civil and Environmental Engineering, Nagaoka University of Technology, 1603-1, Kamitomioka, Nagaoka, Niigata 940-2188, Japan

High-pressure excess adsorption equilibria of methane and carbon dioxide on five microporous activated carbons were measured. Adsorption isotherms were obtained at temperatures ranging from (273 to 333) K and at pressures ranging from (0.5 to 6000) kPa using a static volumetric apparatus. The experimental data were analyzed using the Toth model and the Dubinin−Astakhov model. The isosteric enthalpies of adsorption and the limiting heat of adsorption for both adsorbates on all activated carbons were calculated using the Clausius−Clapeyron equations and the van't Hoff equations, respectively.

Introduction

Physical adsorption on activated carbon and carbonaceous adsorbents is widely used for the separation and purification of gases.[1,2] In recent years, high-pressure adsorption has often been applied in industrial adsorption processes.[3] One significant commercial application is the adsorption of methane during natural gas storage.[4] Adsorbed natural gas is considered to be a better choice for vehicles than compressed natural gas because the adsorption system has the advantage of low storage pressure. The development of efficient natural gas storage capabilities is an important factor in the utilization of natural gas energy. Introduced in Japan, another new application of high-pressure adsorption is as an effective sludge digestion gas (biogas) storage technology. The effective use of biogas is expected to be an efficient way of reducing greenhouse gases. Biogas typically consists of volume fractions of (55 to 65)% methane and (30 to 40)% carbon dioxide and trace components (water, hydrogen sulfide, organic acid, etc). In Japan, biogas generated in a sewage treatment plant is desulfurized and stored in gas holders at pressures up to 0.7 MPa for use as a boiler fuel and for power generation. However, the utilization of biogas is only approximately (60 to 70)%, and the remaining gas is incinerated. More effective utilization would reduce greenhouse gas emissions and encourage the creation of a recycling society. Effective biogas adsorption storage technology is necessary. Furthermore, detailed data of methane and carbon dioxide mixed gas adsorption is also required if separation from landfill gases[5,6] is to be applied. Such gases frequently consist of volume fractions of (50 to 65)% methane and (30 to 40)% carbon dioxide.

The development of such a system of adsorption-based processes requires basic adsorption equilibrium data across a wide range of pressure and temperature. There have been several studies on the adsorption of gases by adsorbents. However, there are relatively few studies on high-pressure adsorption. The adsorption isotherms of appropriate mixtures are also required for the development of biogas adsorption storage and landfill gas separation technologies. Currently, however, adsorption equilibria data of mixed gases are rarely measured. Some multicomponent adsorption equilibrium models are able to predict the adsorption behavior of mixtures using only the adsorption isotherms of pure substances.[7] Hence, it will become necessary to measure precise isotherms for pure substances across a wide range of temperature and pressure.

In this research, an adsorption apparatus based on a static volumetric method was constructed in our laboratory. Results are reported for a systematic study of the adsorption of methane and carbon dioxide on five activated carbons. Experiments were performed at temperatures ranging from (273 to 333) K and pressures up to 6 MPa. Experimental data were correlated by the Toth model and the Dubinin−Astakhov (D−A) model. We also discuss the isosteric enthalpies of adsorption, which are important factors in system performance.

Table 1. Physical Characteristics of Activated Carbons Used This Study

activated carbon	shape	raw material	SBET/ $m^2\ g^{-1}$ [a]	V/cm^{-3} g^{-1} [b]	$d/g\ cm^{-3}$ [c]
Norit R 1 Extra	cylinder	peat	1450	0.47	0.43
BPL	granular	coal	1150	0.43	0.51
Maxsorb	powder	chark	3250	1.79	0.29
A10 fiber		petroleum pitch	1200	0.53	0.20
activated carbon A	crushing	coconut shell	1207	0.54	0.60

[a] BET surface area. [b] Pore volume. [c] Packed density.

Experimental Section

Materials. In this study, we investigated four commercially available activated carbons: Norit R1 Extra (Norit Co.), BPL (Calgon Co.), Maxsorb (Kansai Netsu Kagaku Co.), A10 (A'dall Co.), and an engineering sample (activated carbon A from Osaka Gas Co.). These activated carbons have been used in research on high-pressure methane adsorption. Prior to the experiment, the samples were maintained at a temperature of 433 K in a drying vacuum oven for more than 12 h to remove impurities. The physical properties of these adsorbents were evaluated by measuring the adsorption isotherms of nitrogen at 77 K, and the value of the relative pressure was in the range between (0.01 and 0.99) as measured using an automatic analyzer (AUTOSORB 1200, Yuasa Ionics Co.). The characteristics of all activated carbons are reported in Table 1.

* To whom correspondence should be addressed. E-mail: himeno@vos.nagaokaut.ac.jp. Fax: +81-258-47-9623.

10.1021/je049786x CCC: $30.25
Published on Web 01/25/2005

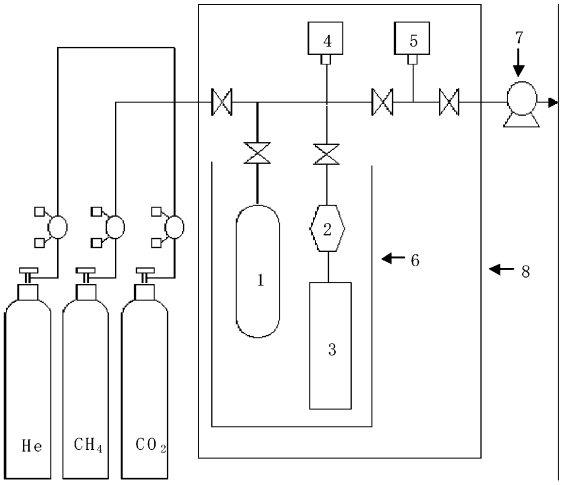

1:Gas cylinder 2:Filter 3:Adsorption cell
4:Pressure gauge (0 to 6.895)MPa 5:Pressure gauge (0 to 66) kPa
6:Water bath 7:Rotary vacuum pump 8:Constant temperature bath

Figure 1. Schematic diagram of the adsorption apparatus used in this study.

The BET specific surface area of Maxsorb was approximately 3250 m^2/g, and that of the other activated carbons was approximately 1250 m^2/g. The total pore volume was determined from the adsorption capacity of liquid nitrogen at the highest relative pressure point. The adsorbates investigated were methane and carbon dioxide (Kaneko Syokai Co.), with purities of 99.99% and 99.9%, respectively.

Apparatus and Procedure. The experimental apparatus used a static volumetric method. A schematic diagram of it is shown in Figure 1. The apparatus was constructed with stainless steel tubes. All lines were 1/4 in i.d., and Swagelok type SS-DLS4 valves were used. A loading cell volume of (72.0 ± 0.1) mL and an adsorption cell volume of (34.3 ± 0.1) mL were the focal points of the apparatus. The cell volumes were measured using helium expansion and the volume of water used to fill the cell. The dead volume was measured using helium expansion. Using the volumetric method, we determined the total amount of gas introduced into the system and that remaining in the system after adsorption equilibrium by $P-V-T$ measurements.

Pressure measurements were made using two Baratron absolute pressure transducers (MKS type 750B) operating in two different pressure ranges. The system temperature outside the two cells was operated to within ±0.1 K uncertainty. During the adsorption experiment, the two cells were placed in a water bath with the temperature maintained constant to within ±0.05 K uncertainty. The uncertainty of the adsorbent mass was ±0.1 mg, and the uncertainty of the adsorbed amount was estimated to be ±(2 to 4)%, which are typical errors found in the volumetric method technique. After the adsorbent was placed in the adsorption cell, it was heated to 533 K under high-vacuum conditions for 2 h using a rotary vacuum pump (Shimadzu type GDH-60).

The adsorbate was introduced into the loading cell, and after the pressure and temperature in the loading cell stabilized, the adsorption step was carried out. The adsorption equilibrium state was considered to have been achieved when the pressure and temperature of the system were constant. This usually occurred within (40 to 60) min, and hence we measured the equilibrium pressure (1.0 to 1.5) h after the initial adsorption. Equilibrium experiments were carried out for all activated carbons at temperatures ranging from (273 to 333) K and pressures up to 6 MPa. To check the accuracy and reproducibility of the experiments, we carried out several runs under identical conditions, obtaining good reproducibility in all cases, with deviations of the amount adsorbed smaller than 5%.

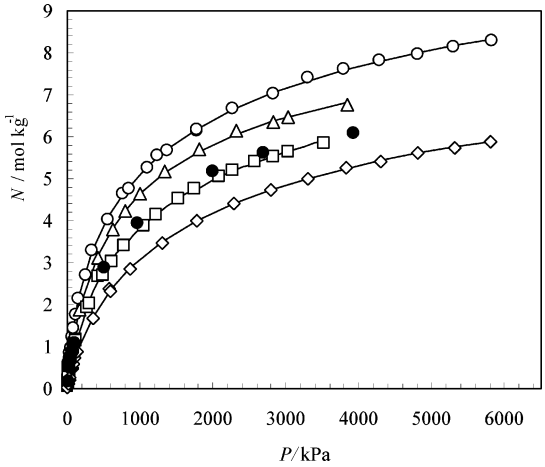

Figure 2. Adsorption isotherms of methane on Norit R1 Extra: ○, 273 K; △, 283 K; □, 298 K; ◊, 323 K; ●, ref 9; solid lines are from the Toth equation fit.

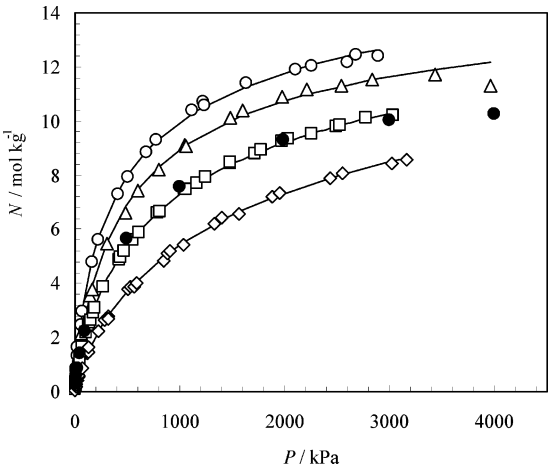

Figure 3. Adsorption isotherms of carbon dioxide on Norit R1 Extra: ○, 273 K; △, 283 K; □, 298 K; ◊, 323 K; ●, ref 9; solid lines are from the Toth equation fit.

Results and Discussion

Adsorption Isotherm. The data for the adsorption of methane and carbon dioxide onto five activated carbons were obtained for temperatures ranging from (273 to 333) K and pressures up to 6 MPa. The experimental data are graphically presented in Figures 2 to 7. The isotherms obtained for methane adsorption on all activated carbons were found to belong to type 1 of the IUPAC classification.[8] In this study, the Gibbs definition of the surface excess amount adsorbed was measured. Maxima were observed in the isotherms of carbon dioxide on Norit R1 Extra and BPL at 283 K and in the isotherm of carbon dioxide on activated carbon A at 298 K at pressures >3.5 MPa.

The adsorption equilibrium of methane and carbon dioxide has been compared with literature data. Our experimental isotherms of methane and carbon dioxide adsorbed on Norit R1 Extra obtained by the volumetric method were compared with the data obtained by the

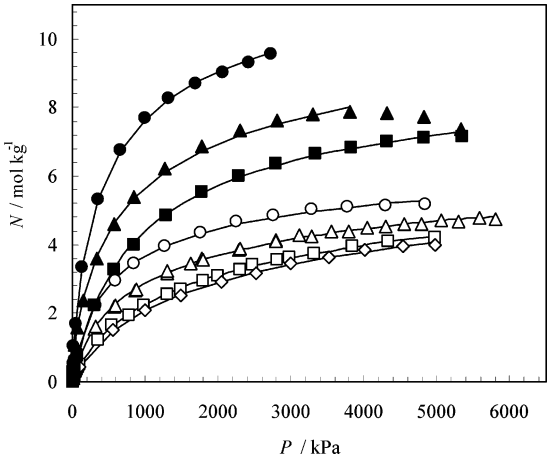

Figure 4. Adsorption isotherms of methane and carbon dioxide on BPL: ○, methane at 273 K; △, methane at 298 K; □, methane at 323 K; ◊, methane at 333 K; ●, carbon dioxide at 273 K; ▲, carbon dioxide at 298 K; ■, carbon dioxide at 323 K; solid lines are from the Toth equation fit.

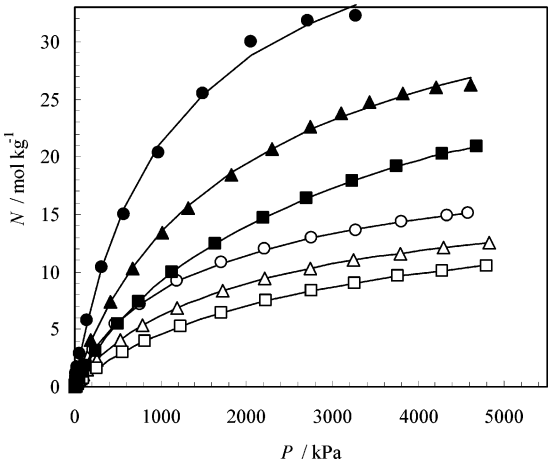

Figure 5. Adsorption isotherms of methane and carbon dioxide on Maxsorb: ○, methane at 273 K; △, methane at 298 K; □, methane at 323 K; ●, carbon dioxide at 273 K; ▲, carbon dioxide at 298 K; ■, carbon dioxide at 323 K; solid lines are from the Toth equation fit.

gravimetric method, taken from the cited literature.[9] These isotherms are in good agreement with the results obtained in this study, and they are graphically presented in Figures 2 and 3. Furthermore, methane and carbon dioxide uptake at 3.5 MPa of four commercially available activated carbons from the cited literature are summarized in Table 2.[9−13] The measurement conditions of pressure, temperature, and adsorbate are also listed. The data on the quantity of methane and carbon dioxide uptake according to our results were also in good agreement with the data from the cited literature.

For all activated carbons within our experimental range, the amount of carbon dioxide adsorbed was about twice that of the methane adsorbed. The adsorption capacity, defined as the amount of adsorbate per gram of adsorbent at the plateau of the isotherm, was highest for Maxsorb. The adsorption capacity is ordered as follows: Maxsorb > activated carbon A > Norit R1 Extra > A10 > BPL. All the carbons used in this study predominantly have micropores (<2 nm) that contribute to the adsorption of methane or carbon dioxide at room temperature. The order of the adsorption capacity of activated carbons was almost the same as the order of the BET surface area and pore volume listed in Table 1.

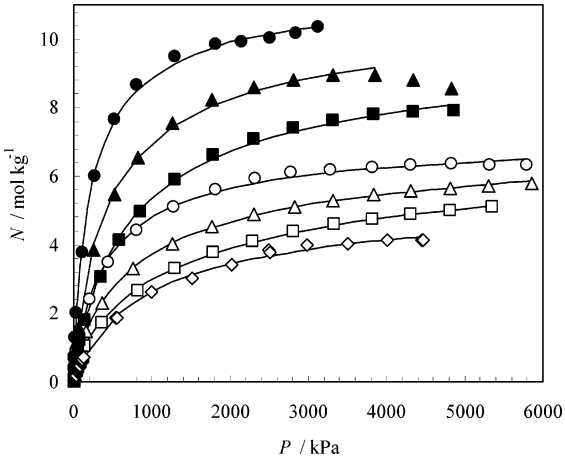

Figure 6. Adsorption isotherms of methane and carbon dioxide on A10: ○, methane at 273 K; △, methane at 298 K; □, methane at 323 K; ◊, methane at 333 K; ●, carbon dioxide at 273 K; ▲, carbon dioxide at 298 K; ■, carbon dioxide at 323 K; solid lines are from the Toth equation fit..

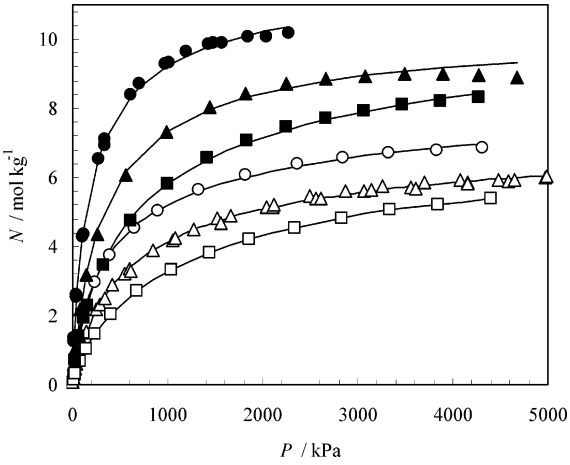

Figure 7. Adsorption isotherms of methane and carbon dioxide on activated carbon A: ○, methane at 273 K; △, methane at 298 K; □, methane at 323 K; ●, carbon dioxide at 273 K; ▲, carbon dioxide at 298 K; ■, carbon dioxide at 323 K; solid lines are from the Toth equation fit.

Table 2. Comparison of Adsorption Equilibrium Measurements from Different Sources

carbon form	adsorbate	N/ mmol g^{-1}	P/MPa	T/K	literature
Norit R1 Extra	methane	6.51	3.93	298	9
	carbon dioxide	10.2	3.99	298	9
BPL	methane	3.79	3.45	unknown	10
	methane	4.05	3.45	301	11
	carbon dioxide	7.28	3.45	301	11
Maxsorb	methane	11.5	3.45	298	12
A10	methane	4.31	3.45	303	13

Correlation of Isotherms. Two different models—those of Toth and Dubinin−Astakhov—have been used to correlate our experimental equilibrium data. The Toth model is commonly used for heterogeneous adsorbents such as activated carbon[14,15] because of its correct behavior at both low and high pressures and the simple form of its equation. The Toth equation can be represented by

$$N = \frac{mP}{(b + P^t)^{1/t}} \tag{1}$$

where N is the amount adsorbed, m is the saturated

amount adsorbed, P is the equilibrium pressure, b is the equilibrium constant, and t is the parameter that indicates the heterogeneity of the adsorbent.

The Dubinin−Astakhov model has been applied to the adsorption equilibria of several vapors and gases onto microporous activated carbons.[16] This model has also been extended to high-pressure adsorption equilibria.[17,18] The D−A equation is written as

$$W = W_0 \exp\left[-\left(\frac{A}{E}\right)^n\right] \tag{2}$$

where W is the volume adsorbed, W_0 is the limiting micropore volume, E is the characteristic energy of the system, n is the heterogeneity parameter, and A is the adsorption potential.

The adsorption potential A is given by

$$A = RT \ln\left(\frac{P_s}{P}\right) \tag{3}$$

where R is the gas constant, T is the equilibrium temperature, and P_s is the saturated pressure.

To apply the D−A equation under supercritical conditions, it is necessary to estimate the density of the adsorbed phase and the saturated vapor pressure (P_s). The adsorbed-phase density D_s is estimated using the following equations[19]

$$D_s = \frac{d_s T_b}{\exp[\alpha(T - T_b)]} \qquad (T > T_b) \tag{4}$$

$$W = \frac{NM}{D_s} \tag{5}$$

where $d_s(T_b)$ is the density of the liquid at the boiling point T_b, α is the thermal expansion of the superheated liquid ($0.0025\ K^{-1}$ was used in this study), and M is the molecular weight.

At high pressure, the pressure should be replaced by the fugacity to correct for the nonideality of gases. Then, the adsorption potential A can be replaced as follows:

$$A = RT \ln\left(\frac{f_s}{f}\right) \tag{6}$$

where f_s is the saturated fugacity at T and f is the equilibrium fugacity.

In the supercritical region, above the critical temperature (T_c) where the concept of vapor pressure no longer holds, the use of pseudovapor pressure has been proposed. For adsorption temperatures T in the supercritical range, the pseudovapor pressures calculated by Dubinin's method were used.[17]

$$P_s = \left(\frac{T}{T_c}\right)^2 P_c \qquad (T > T_c) \tag{7}$$

The saturated fugacities were calculated from the estimated P_s values by the Peng−Robinson equation.[20] The parameters for each model were selected using the Nelder−Mead simplex algorithm. The objective function is

$$\min \sum (N_{exptl} - N_{calcd})^2 \tag{8}$$

where N_{exptl} represents the experimental data of the adsorbed amount and N_{calcd} represents the correlation results. The average deviation ΔN was utilized to compare the correlation results with experimental data,

$$\Delta N = \frac{1}{k}\sum \left|\frac{N_{exptl} - N_{calcd}}{N_{exptl}}\right| \tag{9}$$

where k is the number of data points.

Table 3. Parameters of the Toth Equation for Activated Carbons

		methane				carbon dioxide			
activated carbons	T/K	m/mol kg^{-1}	b/ kPa^t	t	ΔN	m/mol kg^{-1}	b/ kPa^t	t	ΔN
Norit R1 Extra	273	13.64	13.52	0.459	0.014	17.72	19.99	0.570	0.078
	283	10.32	33.44	0.583	0.019	15.38	52.88	0.689	0.045
	298	10.80	27.27	0.525	0.017	16.80	35.19	0.583	0.050
	323	9.743	55.37	0.587	0.012	17.61	47.12	0.565	0.030
BPL	273	6.813	42.84	0.647	0.033	13.70	18.71	0.561	0.084
	298	6.809	49.12	0.616	0.027	12.00	19.38	0.533	0.070
	323	7.686	55.70	0.578	0.023	9.438	163.2	0.770	0.092
	333	7.231	87.08	0.623	0.012				
Maxsorb	273	24.42	102.1	0.665	0.021	47.13	414.6	0.872	0.132
	298	20.35	282.3	0.768	0.045	41.88	472.8	0.827	0.077
	323	19.36	469.2	0.785	0.008	41.80	340.3	0.738	0.034
A10	273	7.338	79.52	0.772	0.053	11.78	41.36	0.749	0.094
	298	7.573	56.03	0.658	0.026	11.07	70.17	0.744	0.095
	323	7.934	44.56	0.586	0.053	10.04	133.95	0.777	0.068
	333	5.587	211.2	0.802	0.039				
activated carbon A	273	8.791	27.11	0.617	0.040	12.22	27.63	0.701	0.025
	298	7.524	75.33	0.717	0.034	10.43	94.06	0.817	0.031
	323	8.496	57.49	0.619	0.012	11.56	37.36	0.617	0.032

The relevant parameters for the Toth equation at different temperatures are listed in Table 3. The solid lines in Figures 2 to 7 denote the adsorption isotherms plotted according to the Toth equation. The Toth equation provided the best fit to the experimental adsorption isotherms of methane and carbon dioxide for all activated carbons in the pressure range below which a maximum occurs. The parameters of the Toth equation have been compared with the literature.[21,22] In the case of methane the adsorption isotherm on BPL at 301 K, the parameters of the Toth equation (m = 6.03, b = 177, t = 0.773) were reported. Values of b in our data and the data in the cited literature appear to be different. However, the isotherms obtained in this study were close to the published data. The differences may be related to the pressure range of the isotherms. Reich et al. measured isotherms in the range of (70 to 3800) kPa, whereas our isotherms were measured in the range of (1 to 6000) kPa.[22] The b parameter indicates the affinity of adsorption at low pressure. Because data have been considered in the low-pressure range in parameter fitting, the value of b from our isotherm differed from the value reported in the literature cited.

The parameters of the D−A equation of all activated carbons are listed in Table 4. Figures 8 to 12 show the characteristic curves for methane and carbon dioxide on all carbon samples. The parameters of the D−A equation for methane on Maxsorb have been previously reported, and the values of W_0, E, and n were 1.09, 5680, and 1.40, respectively.[23] The parameters obtained in this study are in good agreement with these results.

By using the adsorbed phase density and pseudovapor pressure calculated using eqs 4 and 7, we obtained the same characteristic curve at different temperatures. Variously marked points at different temperatures fit the same curve well. Subsequently, high-pressure adsorption isotherms of methane and carbon dioxide showed good correlation with the D−A equation for all activated carbons. In Table 4, it can be observed that the W_0 values for carbon

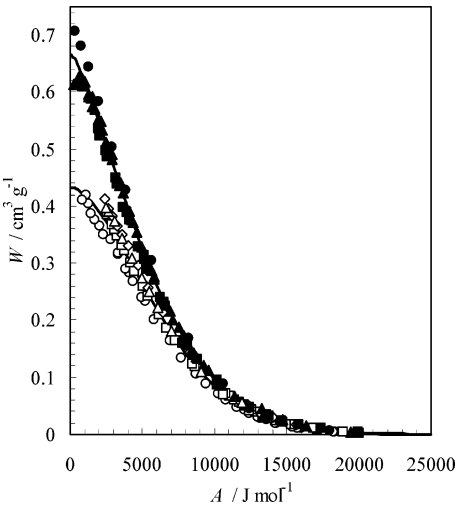

Figure 8. Characteristic curve for methane and carbon dioxide on Norit R1 Extra: ○, methane at 273 K; △, methane at 283 K; □, methane at 298 K; ◊, methane at 323 K; _, carbon dioxide at 273 K; ●, carbon dioxide at 283 K; ▲, carbon dioxide at 298 K; ■, carbon dioxide at 323 K; solid lines are from the D−A equation.

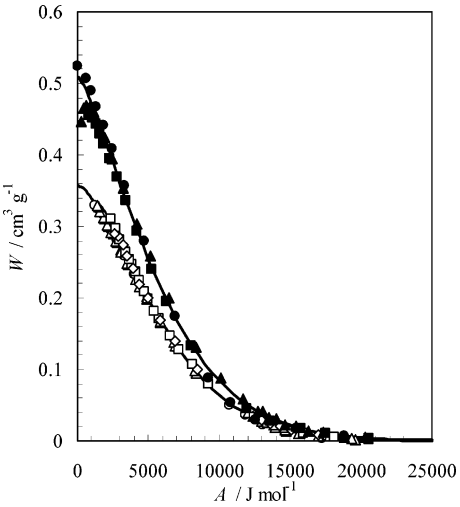

Figure 9. Characteristic curve for methane and carbon dioxide on BPL. ○, methane at 273 K; △, methane at 298 K; □, methane at 323 K; ◊, methane at 333 K; ●, carbon dioxide at 273 K; ▲, carbon dioxide at 298 K; ■, carbon dioxide at 323 K; solid lines are from the D−A equation.

Table 4. Parameters of the Dubinin−Astakhov Equation for Activated Carbons

	W_0/cm^3 g^{-1}	E/J mol^{-1}	n
methane			
Norit R1 Extra	0.43	7500	1.73
BPL	0.36	7040	1.54
Maxsorb	1.12	5220	1.32
A10	0.43	7360	1.51
activated carbon A	0.45	7850	1.64
carbon dioxide			
Norit R1 Extra	0.67	6300	1.43
BPL	0.51	6510	1.38
Maxsorb	1.62	4540	1.31
A10	0.54	7370	1.66
activated carbon A	0.55	7870	1.70

dioxide on all activated carbons were (120−150)% larger than those for methane. The D−A equation can be applied to supercritical gases; it is necessary to define the adsorbed phase density (adsorbed-phase molar volume). In this study, it was estimated by eq 4, proposed by Ozawa et al.[19] We considered that the presumption of the adsorbed-phase

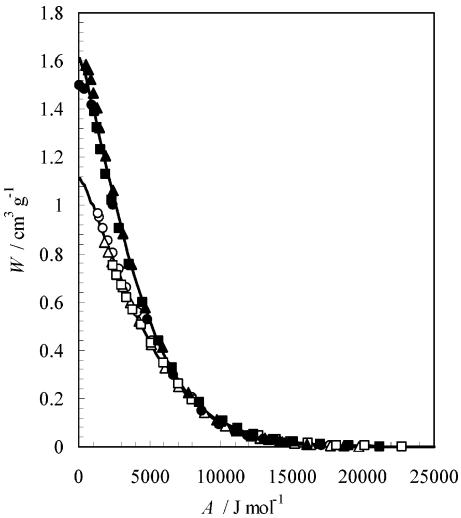

Figure 10. Characteristic curve for methane and carbon dioxide on Maxsorb: ○, methane at 273 K; △, methane at 298 K; □, methane at 323 K; ● carbon dioxide at 273 K; ▲, carbon dioxide at 298 K; ■, carbon dioxide at 323 K; solid lines are from the D−A equation.

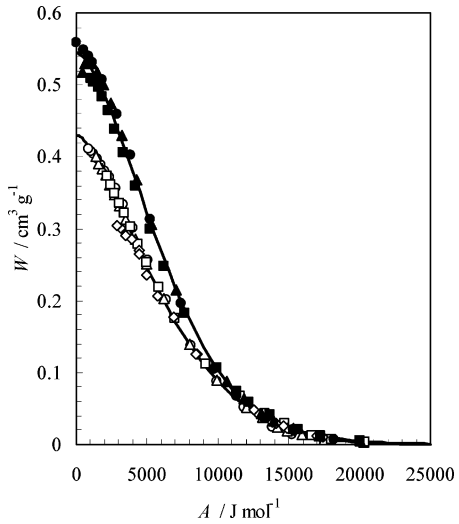

Figure 11. Characteristic curve for methane and carbon dioxide on A10: ○, methane at 273 K; △, methane at 298 K; □, methane at 323 K; ◊, methane at 333 K; ●, carbon dioxide at 273 K; ▲, carbon dioxide at 298 K; ■, carbon dioxide at 323 K; solid lines were D−A equation.

density of methane, which is a supercritical gas, and carbon dioxide, which is a subcritical gas, differed in the case of W_0.

The Toth equation provided a more accurate correlation than the D−A equation. However, because the parameters of the D−A equation are independent of temperature, it is possible to predict the adsorption isotherm at all temperatures for the same gas−solid system, and the D−A equation is effective in evaluating the influence on temperature. Therefore, the two models selected in this study complement each other in engineering design and development.

Henry's Law Constant and Isosteric Enthalpies of Adsorption. The Henry's law constant has been used as a criterion for the affinity of adsorption at low surface coverages. The Henry's law constants were determined by the Toth equation. This equation shows the theoretical limits at pressures approaching zero where it also displays good behavior conforming to Henry's law.[21] The Henry's

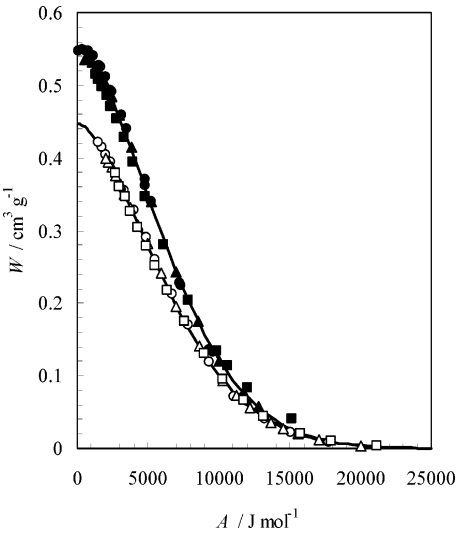

Figure 12. Characteristic curve for methane and carbon dioxide on Activated carbon A. ○, methane at 273 K; △, methane at 298 K; □, methane at 323 K; ●, carbon dioxide at 273 K; ▲, carbon dioxide at 298 K; ■, carbon dioxide at 323 K; solid lines are from the D−A equation.

Table 5. Henry's Law Constants for Activated Carbons

		H/mol kg^{-1} kPa^{-1}	
activated carbons	T/K	methane	carbon dioxide
Norit R1 Extra	273	0.0466	0.0928
	283	0.0251	0.0486
	298	0.0200	0.0373
	323	0.0104	0.0193
BPL	273	0.0204	0.0741
	298	0.0122	0.0459
	323	0.0073	0.0126
	333	0.0056	
Maxsorb	273	0.0232	0.0468
	298	0.0131	0.0244
	323	0.0076	0.0155
A10	273	0.0253	0.0818
	298	0.0167	0.0365
	323	0.0122	0.0184
	333	0.0071	
activated carbon A	273	0.0418	0.1074
	298	0.0181	0.0401
	323	0.0122	0.0326

Table 6. Henry's Law Constants for BPL from Different Sources

T/K	H/mol kg^{-1} kPa^{-1}	literature
	Methane	
301	0.0078	22, 23
	Carbon Dioxide	
303	0.052	22, 26
313	0.045	22, 26
323	0.027	22, 26

law constants for all activated carbons at different temperatures are listed in Table 5. The Henry's law constant is also determined by the extrapolation of isothermal ln(P/N) versus N data to zero adsorbed concentration.[24] The values of the Henry's law constants obtained by both methods were in agreement.

The Henry's law constants of methane and carbon dioxide on BPL, taken from the cited literature, are given in Table 6.[21,22,25] The Henry's law constants of methane are close to the values obtained from our results. However, the values of the Henry's law constants of carbon dioxide are slightly larger than those obtained from our data. These differences are probably related to the pressure range of

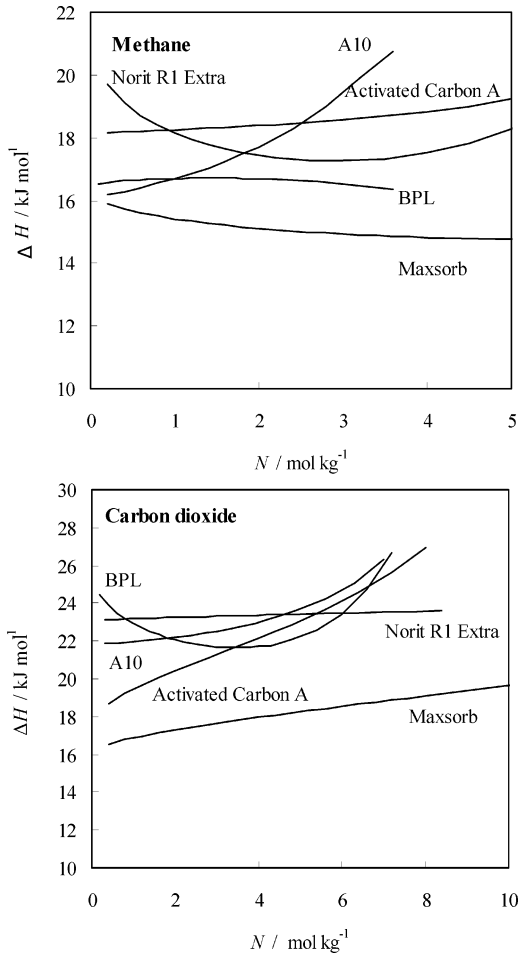

Figure 13. Isosteric enthalpies of adsorption for methane and carbon dioxide on activated carbons.

the isotherms. Meredith et al. plotted isotherms at pressures below 100 kPa, whereas our isotherms were plotted at pressures up to 6 MPa. The Henry's law constants of carbon dioxide in all activated carbons were approximately 2 to 3 times higher than those of methane. Values of the Henry's law constant for the activated carbons are in the following order: Norit R1 Extra > Activated Carbon A > A10 > Maxsorb > BPL.

If the adsorption is ideal, then the heat of adsorption will be independent of the adsorbed loading. However, because many adsorbents such as activated carbon have energetically heterogeneous surfaces, the heat of adsorption affects the adsorption performance of the process.The isosteric enthalpy of adsorption is generally applied to characterize the influence of the heat of adsorption on an adsorbent.

The isosteric enthalpy of adsorption is calculated by the Clausius−Clapeyron equation applied to adsorption:[26]

$$\frac{\Delta H}{RT^2} = -\left[\frac{\partial \ln P}{\partial T}\right]_N \tag{10}$$

where ΔH is the isosteric enthalpy of adsorption.

In Figure 13, the isosteric enthalpies of adsorption for our two adsorbates are plotted as a function of the amount of gas adsorbed during loading. As shown in this Figure, the isosteric enthalpy of adsorption varied with the surface loading. In a ranking of the adsorbents on the basis of isosteric enthalpies of adsorption at low loading, Norit R1 Extra is the highest, and Maxsorb is the lowest. This is because the heat of adsorption at low surface coverage is

Table 7. Limiting Heat of Adsorption for Activated Carbons

	ΔH/kJ mol^{-1}	
activated carbons	methane	carbon dioxide
Norit R1 Extra	20.6	22.0
BPL	16.1	25.7
Maxsorb	16.3	16.2
A10	16.2	21.6
activated carbon A	18.3	17.8

related to the interaction between the adsorbent surface and adsorptive molecular forces.[27] The value of the isosteric enthalpy of adsorption at low surface coverage is related to the pore size of the activated carbon, and the value of Maxsorb is the lowest because it has the largest average pore diameter among all of the activated carbons used in this study. As shown in Table 5, the Henry's law constants indicate that the adsorption affinity at low surface coverage was highest for Norit R1 Extra and lowest for Maxsorb.

The isosteric enthalpies of adsorption of methane for BPL, Maxsorb, and activated carbon A and the isosteric enthalpies of adsorption of carbon dioxide for Norit R1 Extra increase or decrease slightly as the loading increases. This indicates a homogeneous adsorption system although the trends are well within experimental uncertainty. The isosteric enthalpies of adsorption of methane for A10 and carbon dioxide for Maxsorb, A10, and activated carbon A increase more substantially with an increase in the loading. This suggests that adsorbate interactions are becoming more significant. The isosteric enthalpies of adsorption of methane for Norit R1 Extra and that of carbon dioxide for BPL decrease and then increase. This indicates that energetic heterogeneity is the main initial effect at low coverage and that the interaction between the adsorbates begins to dominate as the amount adsorbed increases.

The limiting heat of adsorption at zero coverage, as calculated from the slopes of the van't Hoff plots of the Henry's law constants against the inverse temperature,[28] is listed in Table 7. The limiting heat of adsorption at zero coverage for methane in BPL was evaluated by comparing it with the values in the cited literature, and it has been reported to range from (17.8 and 20.8) kJ mol^{-1}.[21,25] The values in our data appear to be slightly lower than the values in the cited literature. This difference may be related to the calculation method; our value was calculated from the slope of the van't Hoff plots, and the values in the cited literature were calculated using the Toth and the UNILAN equations.[21] The values of the limiting heat of adsorption listed in Table 7 are in good agreement with the values determined by the extrapolation of the isosteric enthalpies of adsorption. The limiting heat of adsorption reflects the strength of the interaction between adsorbate molecules and adsorbent atoms.

Conclusions

Adsorption isotherms were plotted for methane and carbon dioxide adsorbed on five activated carbons at temperatures ranging from (273 to 333) K and at pressures ranging from (0.01 to 6000) kPa. The adsorption data of Norit R1 Extra were found to be in good agreement with the data reported by other research groups. The maxima in the "Gibbs surface excess amount" were observed in the carbon dioxide isotherms at pressures >3.5 MPa. The experimental equilibrium data for methane and carbon dioxide were correlated with the Toth equations and the Dubinin−Astakhov equations in the pressure range below which a maximum occurs.

The isosteric enthalpies of adsorptions were calculated using the Clausius−Clapeyron equation, resulting in the conclusion that the activated carbons have energetically heterogeneous surfaces. The dependence of the changes in the heat of adsorption and the thermal effects on the nature and source of the activated carbons studied underlines their importance when selecting activated carbons for specific purposes.

Literature Cited

(1) Yang, R. T. *Gas Separation by Adsorption Processes*; Butterworths: Boston, 1987.

(2) Ruthven, D. M. *Principles of Adsorption and Adsorption Processes*; John Wiley & Sons: New York, 1984.

(3) Sircar, S.; Golden, T. C.; Rao, M. B. Activated Carbon for Gas Separation and Storage. *Carbon* **1996**, *34*, 1−12.

(4) Talu, O. An Overview of Adsorptive Storage of Natural Gas. *Fundamentals of Adsorption 5*; Kodansha: Tokyo, 1993; pp 655−662.

(5) Sircar, S. Separation of Methane and Carbon Dioxide Gas Mixtures by Pressure Swing Adsorption. *Sep. Sci. Technol.* **1988**, *23*, 519−529.

(6) Kapoor, A.; Yang, R. T. Kinetic Separation of Methane-Carbon Dioxide Mixture by Adsorption on Molecular Sieve Carbon. *Chem. Eng. Sci*. **1989**, *44*, 1723−1783.

(7) Ahmadpour, A.; Wang, K.; Do, D. D. Comparison of Models on the Prediction of Binary Equilibrium Data of Activated Carbons. *AIChE J*. **1998**, *44*, 740−752.

(8) Sing, K. S. W.; Everett, D. H.; Haul, R. A. W.; Moscoul, L.; Pierotti, R. A.; Rouqerol, J.; Siemieniewska, T. Reporting Physisorption Data for Gas/Solid Systems with Special Reference to the Determination of Surface Area and Porosity. *Pure Appl. Chem.* **1985**, *57*, 603−619.

(9) Dreisbach, F.; Staudt, R.; Keller, J. U. High-Pressure Adsorption Data of Methane, Nitrogen, Carbon Dioxide and their Binary and Ternary Mixtures on Activated Carbon. *Adsorption* **1999**, *5*, 215−227.

(10) Sun, J.; Brady, T. A.; Rood, M. J.; Lebmann, C. M.; Rostam-Abady, M.; Lizzio, A. A. Adsorbed Natural Gas Storage with Activated Carbons Made from Illinois Coals and Scrap Tires. *Energy Fuels* **1997**, *11*, 316−322.

(11) Hines, A. L.; Kuo, S.-L.; Dural, N. H. A New Analytical Isotherm Equation for Adsorption on Heterogeneous Adsorbents. *Sep. Sci. Technol.* **1990**, *25*, 869−888.

(12) Lozano-Castello, D.; Cazorla-Amoros, D.; Linares-Solano, A. Powdered Activated Carbons and Activated Carbon Fibers for Methane Storage: A Comparative Study. *Energy Fuels* **2002**, *16*, 1321−1328.

(13) New Energy and Industrial Technology Development Organization. Characteristics and Preparations of Porous Carbons for Energy Storage; NEDO-GET-9951, 2000 (in Japanese).

(14) Toth, J. *Adsorption: Theory, Modeling, and Analysis*; Marcel Dekker: New York, 2002.

(15) Yun, J.-H.; Choi, D.-K.; Kim, S.-H. Adsorption Equilibria of Chlorinatedorganic Solvents onto Activated Carbons. *Ind. Eng. Chem. Res.* **1998**, *37*, 1442−1427.

(16) Dubinin, M. M. Generalization of the Theory of Volume Filling of Micropores to Nonhomgeneous Microporous Structures. *Carbon* **1985**, *23*, 373−380.

(17) Amankwah, K. A. G.; Schwarz, J. A. A modified approach for estimating pseudo vapor pressures in the application of the Dubinin-Astakhov equation. *Carbon* **1995**, *33*, 1313−1319.

(18) Sievers, W.; Mersmann, A. Single and multicomponent adsorption equilibria of carbon dioxide, nitrogen, carbon monoxide and methane in hydrogen purification processes. *Chem. Eng. Technol*. **1994**, *17*, 324−337.

(19) Ozawa, S.; Kusumi, S.; Ogino, Y. Physical adsorption of gases at high pressure. An improvement of the Dubinin-Astakhov equation. *J. Colloid. Interface Sci*. **1976**, *56*, 83−91.

(20) Elliott, J. R.; Lira C. T. *Introductory Chemical Engineering Thermodynamics*; Prentice Hall PTR: Upper Saddle River, NJ, 1999.

(21) Valenzuela, D. P.; Myers, A. L. *Adsorption Equilibrium Data Handbook*; Prentice-Hall: Englewood Cliffs, NJ, 1989.

(22) Reich, R.; Ziegler, W. T.; Rogers, K. A. Adsorption of Methane, Ethane, and Ethylene Gases and Their Binary and Ternary Mixtures and Carbon Dioxide on Activated Carbon at 212−301 K and Pressure to 35 Atmospheres. *Ind. Eng. Chem. Process Des. Dev*. **1980**, *19*, 336−344.

(23) Biloe, S.; Goetz, V.; Guillot, A. Optimal Design of an Activated Carbon for an Adsorbed Natural Gas Storage System. *Carbon* **2002**, *40*, 1295−1308.

(24) Yang, S.-Y.; Talu, O.; Hayhurst, D. T. High-Pressure Adsorption of Methane in NaX, MgX, CaX, SrX, and BaX. *J. Phys. Chem*. **1991**, *95*, 1722−1726.
(25) Meredith, J. M.; Plank, C. A. Adsorption of Carbon Dioxide and Nitrogen on Charcoal at 30° to 50° C. *J. Chem. Eng. Data*. **1967**, *12*, 259−261.
(26) Young, D. M.; Crowell, A. D. *Physical Adsorption of Gases*; Butterworths: London, 1962.
(27) Nguyen, C.; Do, D. D. Adsorption of Supercritical Gases in Porous Media: Determination of Micropore Size Distribution. *J. Phys. Chem B* **1999**, *103*, 6900−6908.
(28) Sun, M. S.; Shah, D. B.; Xu, H. H.; Talu, O. Adsorption Equilibria of C_1 to C_4 Alkanes, CO_2, and SF_6 on Silicalite. *J. Phys. Chem. B* **1998**, *102*, 1466−1473.

Received for review June 5, 2004. Accepted November 4, 2004. This work was funded by a Grant-in-Aid for Scientific Research B from the Japanese Government and a Grant for Environmental Research Projects from the Sumitomo Foundation.

JE049786X